

Study of Gauged Lepton Symmetry Signatures at Colliders

We-Fu Chang^{1,2} and John N. Ng²

¹*Department of Physics, National Tsing Hua University, Hsinchu 30013, Taiwan*

²*Theory Group, TRIUMF, Vancouver, B.C. V6T2A3, Canada*

(Dated: October 16, 2018)

We construct a new gauged $U(1)_l$ lepton number model which is anomaly free for each SM generation. The active neutrino masses are radiatively generated with a minimal scalar sector. The phenomenology and collider signals are studied. The interference effects among the new gauge boson, Z_ℓ , photon, and Z -boson can be probed at the future e^+e^- colliders even the center-of-mass energy is below the mass of Z_ℓ . Moreover, the electroweak precision sets a stringent bound on the mass splitting of the new lepton doublets.

I. INTRODUCTION

It is well known that the standard model (SM) Lagrangian has an accidental global symmetry associated with the conservation of total lepton number. Equally well known is that the minimal SM cannot accommodate the evidence of active neutrino masses from the neutrino oscillations data. If one allows the dimension five Weinberg operator (Wo)[1] of the form $\frac{c}{\Lambda}LLHH$ where L is the lefthanded lepton doublet, H denotes the Higgs field, Λ is an unknown high scale and c is a free parameter, then after spontaneous symmetry where H takes on a vacuum expectation value $v \simeq 247$ GeV we get a neutrino mass $m_\nu \sim \frac{cv^2}{\Lambda}$. Since data indicate that $m_\nu \lesssim 1$ eV the scale Λ can range from 1 to 10^{11} TeV depending on the value of c . If the neutrinos masses do indeed originate from the Weinberg operator it fortifies the view that the SM is an effective field theory with a small violation of total lepton number in the form of the non-renormalizable Wo.

The Wo gives an elegant explanation for neutrinos masses within the SM. However, its origin is not known and is the subject of the vast field of neutrino mass models. Furthermore, whether the lepton number is a global symmetry or a gauged symmetry and how the symmetry is broken are all open questions. The answers or even partial answers to these questions will add immensely to our understanding of fundamental physics. The simplest way to extend the SM and obtain the Wo is to have two or more SM singlet righthanded (RH) neutrinos N_R . These singlet neutrinos can be given heavy Majorana mass terms that change two units of lepton number explicitly by hand. Integrating these fields out will yield the Wo at low energies which is the well known type I seesaw mechanism[2]. Instead of adding Majorana masses by hand it is theoretically and phenomenologically more interesting to generate them by the spontaneous symmetry breaking (SSB) mechanism. To this end one adds a SM singlet scalar field Φ and form the term $\Phi \overline{N_R^c} N_R$. When Φ gets a vacuum expectation value (VEV) $\langle \Phi \rangle \gg v$, one again gets the Type I seesaw. If the lepton symmetry that is broken is a $U(1)$ global symmetry then a singlet scalar Majoron will exist in the physical spectrum and can act as extra dark radiation [3]. An extended model with a dark matter candidate has also been constructed

in [4] and [5]. Moreover, this symmetry can also be a local gauge symmetry.

The study of the lepton number being a local gauge symmetry has long history. If the symmetry is unbroken one would have a leptonic photon [6]. The corresponding long range force can be searched for in equivalence principle tests [7] and the limit on the leptonic fine structure constant is $\alpha_l < 10^{-49}$. However, a complete and consistent model was not studied until recently in [8] in conjunction with gauged baryon number. Gauging lepton number only is given in [9] where active neutrino masses are given by the usual type I seesaw model. A different implementation with type-II seesaw mechanism[10] is given in [11]. Also there the emphasis is on constructing a consistent dark matter model with gauged lepton number. More recently, a gauged $SU(2)_\ell$ model was considered by[12] with emphasis on producing a dark matter candidate and baryogenesis.

In this work we study a model of gauged lepton number $U(1)_l$ without employing type I seesaw mechanism for active neutrino masses. Specifically, the model does not have SM singlet neutrinos. The SM leptons are assigned lepton number $\ell = 1$, and $U(1)_l$ is spontaneously broken. The existence of lepton specific gauge boson Z_l is a robust prediction of this class of models. The SM is anomalous under $U(1)_l$ and hence new chiral fermions will have to be added. Our solution differs from that of Ref.[9] where they use a set of fermions to solve the anomalies from all three SM lepton families together. We choose to solve the anomaly of the SM leptons within each family and we do not have SM singlet neutrinos as mentioned before.

It is well known that given two $U(1)$ gauge symmetries their corresponding gauge bosons can have kinetic mixing [13] as well as mass mixing. Both are expected to be small. The phenomenology of a kinetically mixed Z' with $U(1)_Y$ gauge boson was given in [14]. In this paper, we shall neglect these mixings.

This paper is organized as follows. In Sec II we discuss the anomalies cancelation solution and the new chiral fermions. Sec. III constructs the Yukawa interactions and the minimal set of scalars required. The scalar potential that leads to symmetry breaking is also constructed. A discussion of charged lepton masses of the model is given in Sec. IV and the extended gauge interactions are

described in Sec V. Particular attention is given to Z_l which must exist in these models independent of which solution to the anomalies one adopts. It is natural to assume that the SM charged leptons has lepton number of one unit the rich phenomenology of Z_l at lepton colliders past and future is guaranteed. Even if its mass denoted by M_X is too heavy to be produced at these colliders its interference with the SM γ and Z can be detected in precision measurements. Such effects are proportional to $\frac{1}{M_X^2}$ and thus sensitive to low mass Z_l . These are discussed in Sec. VI. The production at the LHC is also given there. Since Z_l couples only to leptons and not quarks the search strategy will have to be different from the usual extra Z boson searches. This is followed by a discussion of the phenomenology of the new fermions. Active neutrino masses are generated by 1-loop effect and is given in Sec. VIII. Since it is not the purpose of this paper to do detail neutrino oscillation study we will only present orders of magnitude estimates. Our conclusions are given in Sec. IX.

II. ANOMALIES CANCELATIONS

We extend the SM gauge group by $U(1)_I$; explicitly, it is $G = G_{\text{SM}} \times U(1)_I = SU(2) \times U(1)_Y \times U(1)_I$. The color $SU(3)$ group plays no role here and can be neglected. We define the SM leptons to have number $\ell = 1$ under $U(1)_I$. The new anomaly coefficients for a single SM lepton family are

$$\mathcal{A}_1([SU(2)]^2 U(1)_I) = -1/2, \quad (1a)$$

$$\mathcal{A}_2([U(1)_Y]^2 U(1)_I) = 1/2, \quad (1b)$$

$$\mathcal{A}_3([U(1)_Y][U(1)_I]^2) = 0, \quad (1c)$$

$$\mathcal{A}_4([U(1)_I]^3) = -1, \quad (1d)$$

$$\mathcal{A}_5(U(1)_I) = -1, \quad (1e)$$

where \mathcal{A}_5 is for lepton-graviton anomaly. We also need to check the SM anomalies of $\mathcal{A}_6([SU(2)]^2 U(1)_Y)$, $\mathcal{A}_7([U(1)_Y]^3)$ and $\mathcal{A}_8(U(1)_Y)$ are canceled when new chiral leptons are introduced to cancel Eq.(1).

We introduce two sets of chiral leptons very similar to the SM leptons. The first set consist of a $SU(2)$ doublet and a singlet and has the eigenvalue ℓ_1 . Explicitly we write

$$\begin{aligned} L_{1L} &= (N_{1L}, E_{1L}); \left[\mathbf{2}, -\frac{1}{2}, \ell_1 \right], \\ E_{1R} &; \left[\mathbf{1}, -1, \ell_1 \right], \end{aligned} \quad (2)$$

where the subscript $L(R)$ stands for left(right)-handed projections. The square parenthesis [...] denotes $SU(2), U(1)_Y, U(1)_I$ assignments. A second set with righthanded projections but lepton number ℓ_2 is given by

$$\begin{aligned} L_{2R} &= (N_{2R}, E_{2R}); \left[\mathbf{2}, -\frac{1}{2}, \ell_2 \right], \\ E_{2L} &; \left[\mathbf{1}, -1, \ell_2 \right]. \end{aligned} \quad (3)$$

It is easy to see that Eqs.(1) become

$$\mathcal{A}_1 = -\frac{1}{2}(\ell_1 - \ell_2 + 1), \quad (4a)$$

$$\mathcal{A}_2 = \frac{1}{2}(\ell_1 - \ell_2 + 1), \quad (4b)$$

$$\mathcal{A}_3 = 0, \quad (4c)$$

$$\mathcal{A}_4 = -\ell_1^3 + \ell_2^3 - 1, \quad (4d)$$

$$\mathcal{A}_5 = -(\ell_1 - \ell_2 + 1). \quad (4e)$$

$\mathcal{A}_{1,2,5} = 0$ for $\ell_2 = \ell_1 + 1$. Substituting into $\mathcal{A}_4 = 0$ gives

$$\ell_1(\ell_1 + 1) = 0. \quad (5)$$

The two solutions are

- Solution I

$$\ell_1 = -1 \text{ and } \ell_2 = 0, \quad (6)$$

- Solution II

$$\ell_1 = 0 \text{ and } \ell_2 = 1. \quad (7)$$

It is easy to check that the solutions do not contribute to $\mathcal{A}_{6,7,8}$. This is not surprising since both Eqs.(2,3) form vectorlike pairs under G_{SM} . Thus, Eqs.(6,7) are anomalies free without the use of singlet RH neutrinos.

III. YUKAWA INTERACTIONS

After determining the anomalies free lepton representations we can proceed to construct G invariant Yukawa interactions. This will produce the minimal scalar fields required for viable charged and neutral lepton mass matrices at the tree level.

We will give a detail discussion of the physics associated with solution (I) ¹. The complete set of leptons for this solution and their gauge quantum numbers are given in Table(I). With this, one can form all possible Lorentz invariant bilepton combinations that are invariant under G_{SM} . The next step is to identify scalar fields that will make Yukawa interactions that are invariant under the full gauge group G . Besides the SM Higgs field H_0 , the minimum set of new scalars we require are Φ, S , and H_1 and their quantum numbers are also given in Table(II).

With this, the Yukawa interactions are given by²

$$\begin{aligned} \mathcal{L}_y &= y_e \bar{\ell}_L e_R H_0 + Y_2 \bar{L}_{1L} E_{1R} H_0 + Y_3 \bar{L}_{2R} E_{2L} H_0 \\ &+ \lambda_1 \bar{\ell}_L L_{2R} \Phi_1 + \lambda_2 \bar{E}_{2L} e_R \Phi_1^\dagger + \lambda_3 \bar{L}_{1L} L_{2R} \Phi_1^* \\ &+ \lambda_4 \bar{E}_{2L} E_{1R} \Phi_1 + Y_1 \bar{\ell}_L H_1 E_{1R} + f \bar{\ell}_L^c \epsilon L_{1L} S \\ &+ h.c. \end{aligned} \quad (8)$$

¹ Solution II gives qualitatively the same physics. It is easy to extend our discussions to this case.

² We are interested in the minimal setup. In general there could also be a Yukawa term $\bar{L}_{1L} e_R H_2$ with a second doublet $H_2 : (2, 1/2, -2)$.

Field	$SU(2)$	Y	ℓ
$\ell_L = \begin{pmatrix} \nu_L \\ e_L \end{pmatrix}$	2	$-\frac{1}{2}$	1
e_R	1	-1	1
$L_{1L} = \begin{pmatrix} N_{1L} \\ E_{1L} \end{pmatrix}$	2	$-\frac{1}{2}$	-1
E_{1R}	1	-1	-1
$L_{2R} = \begin{pmatrix} N_{2R} \\ E_{2R} \end{pmatrix}$	2	$-\frac{1}{2}$	0
E_{2L}	1	-1	0

TABLE I. Lepton fields for anomalies free solution I

Field	$SU(2)$	Y	ℓ
$H_0 = \begin{pmatrix} 0 \\ \frac{v+h}{\sqrt{2}} \end{pmatrix}$	2	$\frac{1}{2}$	0
$H_1 = \begin{pmatrix} H_1^+ \\ H_1^0 \end{pmatrix}$	2	$\frac{1}{2}$	2
S	1	1	0
Φ_1	1	0	1
Φ_2	1	0	2

TABLE II. Minimal scalar fields for leptons of solution I

It can be seen that S is charged and cannot develop a VEV. H_1 is a Higgs-like field and may or may not pick up a VEV depending on the parameters in the scalar potential. Here we make the reasonable assumption that the lepton number breaking scale is much higher than v . In order not to have a weak scale lepton number violation we will work in the parameter space where H_1 is not Higgsed since it has $\ell = 2$. Moreover, Φ_1 is a neutral scalar and it can pick up a VEV w and thus can bestow masses to the new charged leptons $E_{1,2}$. They will be much heavier than SM charged leptons if $w \gg v$. Another electroweak singlet scalar Φ_2 with 2 units of lepton number is required for neutrino mass generation as we shall see later. But it does not enter in Eq.(8). We will not include scalar fields with $|Y| > 1$ as they play no role in our study.

Having specified all the necessary scalars, the minimal

G invariant scalar potential is given by

$$\begin{aligned}
V(H_0, H_1, \Phi_1, \Phi_2, S) = & \\
& -\mu^2 H_0^\dagger H_0 + m_1^2 H_1^\dagger H_1 + \kappa_0 (H_0^\dagger H_0)^2 + \kappa_1 (H_1^\dagger H_1)^2 \\
& + \kappa_2 (H_0^\dagger H_0) (H_1^\dagger H_1) + \kappa_3 (H_0^\dagger H_1) (H_1^\dagger H_0) \\
& + m_S^2 S^\dagger S + \kappa_S (S^\dagger S)^2 - \sum_{i=1,2} \mu_i^2 \Phi_i^\dagger \Phi_i \\
& + \kappa_{11} (\Phi_1^\dagger \Phi_1) (\Phi_1^\dagger \Phi_1) + \kappa_{12} (\Phi_1^\dagger \Phi_1) (\Phi_2^\dagger \Phi_2) \\
& + \kappa_{22} (\Phi_2^\dagger \Phi_2) (\Phi_2^\dagger \Phi_2) \\
& + \sum_{i=1,2} \sum_{j=0,1} \kappa_{\Phi_i H_j} (\Phi_i^\dagger \Phi_i) (H_j^\dagger H_j) \\
& + \sum_{i=1,2} \kappa_{\Phi_i S} (\Phi_i^\dagger \Phi_i) (S^\dagger S) + \sum_{i=0,1,2} \kappa_{H_i S} (H_i^\dagger H_i) (S^\dagger S) \\
& + \lambda_{1\ell} H_1 \epsilon H_0 S^\dagger \Phi_2^\dagger + \lambda_{2\ell} H_0^\dagger H_1 (\Phi_1^*)^2 \\
& + \mu_3 H_0^\dagger H_1 \Phi_2^* + \mu_4 (\Phi_1^*)^2 \Phi_2 + h.c.
\end{aligned} \tag{9}$$

Lepton number violation occurs spontaneously for $\langle |\Phi_{1,2}| \rangle = w/\sqrt{2} \neq 0$ and is the only such scale in the model³. Thus, we write $\Phi_{1(2)} = \frac{w+\varphi_{1,(2)}}{\sqrt{2}}$.

After SSB, the lepton mass matrices arise from Eq.(8). The charged lepton matrix in the basis $\mathcal{E} = (e_w, E_1, E_2)^4$ is

$$M_E = \frac{w}{\sqrt{2}} \begin{pmatrix} y_{er} & 0 & \lambda_2 \\ 0 & Y_{2r} & \lambda_4 \\ \lambda_1 & \lambda_3 & Y_{3r} \end{pmatrix} \tag{10}$$

where $r \equiv \frac{v}{w} \ll 1$. And the neutral lepton mass matrix in terms of the chiral states $(\nu_L^w, N_{1L}, N_{2R}^c)^5$ is

$$M_N = \frac{w}{\sqrt{2}} \begin{pmatrix} 0 & 0 & \lambda_1 \\ 0 & 0 & \lambda_3 \\ \lambda_1 & \lambda_3 & 0 \end{pmatrix}. \tag{11}$$

The identity $\bar{\psi}_1^c (\hat{L}/\hat{R}) \psi_2^c = \bar{\psi}_2 (\hat{L}/\hat{R}) \psi_1$ has been used to give the symmetric M_N which is a tree level result. At this level the active neutrino is massless.

However, what is interesting is that Eq.(9) has sufficient structure to give a 1-loop radiative Majorana mass to ν_L^w ; i.e. the upper leftmost entry of Eq.(11) will have a quantum contribution. The source comes from the term involving $\lambda_{2\ell}$ which spontaneously breaks lepton symmetry when Φ_2 gets a VEV. It also induces a mixing

³ In general Φ_1 and Φ_2 need not have the same VEV. This only adds more parameters to the model without adding more physics. We shall assume they are equal.

⁴ Here we introduce the intermediary subscript w to e to remind us it is the weak basis.

⁵ Again the intermediary superscript w is introduced for neutrino.

between the charged scalars H_1^+ and S^+ . The details of radiatively generated active neutrino masses will be discussed in a later section.

Eq.(8) holds for a single lepton family. It can be generalized to the 3 families case by promoting the couplings $y_e, Y_{1,2,3}, \lambda_{1,\dots,4}, f$ to 3×3 matrices. There are also similar terms connecting different families which we will neglect since we are not interested in charged lepton flavor violation or flavor changing neutral current processes in this paper. Henceforth, our discussions will mostly involve only a single lepton family which is designated as the electron family.

A. A quartet of scalar fields

It is easy to see from Eq.(9) that the SM Higgs field in the gauge basis can be identified with H_0 . The SM Higgs field will mix with the real parts of the SM singlets $\Re\Phi_{1,2}$ and SM doublet charge neutral part $\Re H_1^0$ through the quartic couplings $\lambda_{2\ell}, \lambda_{\Phi_1 H_0}, \lambda_{\Phi_2 H_0}$, and the cubic term μ_3 after SSB. The scalar mass matrix is in general 4×4 . We denote this quartet of gauge states by $\mathcal{H}_\alpha = \frac{1}{\sqrt{2}}(\Re H_0^0, \Re H_1^0, \Re\Phi_1, \Re\Phi_2)$. As usual the mass eigenstates $\mathfrak{h}_i = (h_0, h_1, h_2, h_3)$ are related to \mathcal{H} via $\mathfrak{h} = U\mathcal{H}$ where U is a 4×4 unitary mixing matrix. The strength of the mixings given by the elements $U_{i\alpha}$ will depend on the physical masses of the new scalars and the quartic couplings. Since no beyond SM scalars are found at the LHC, we make the conservative assumption that they are all heavier than 800 GeV. However, we are mindful that optimal search strategy for a specific scalar is model dependent. Nevertheless, a robust prediction is that a universal suppression factor U_{11} applies to all SM Higgs couplings which can be probed by the Higgs signal strengths at the LHC. The SM signal strength is parameterized by μ and is unity for the SM. The LHC-1 bound is $\mu = 1.09 \pm 0.11$ [15]. This implies $|U_{11}|^2 > .87$ at 2σ level. Hence, the mixing of H_0 with any of the other three scalars must be quite small or even vanishing. Small mixings can be achieved by tuning the couplings $\lambda_{2\ell}, \lambda_{\Phi_1 H_0}, \lambda_{\Phi_2 H_0}$, and μ_3 .

B. Two simplified cases of lepton mass diagonalization

To capture the physics essence of this model, we will avoid the complication of keeping track of all the free parameters and focus on two simplified scenarios:

- **Scenario-A:** We take $\lambda_{2\ell}$ and μ_3 to be small but finite and we also assume that $Y_2 \sim Y_3 \sim Y$ and $\lambda_{1,2,3,4} \sim \bar{\lambda}$.
- **Scenario-B:** This is the limiting case of $\lambda_{1,2} = 0 = \mu_3$. We also assume that $Y_2 \sim Y_3 \sim Y$ and $\lambda_{3,4} \sim \bar{\lambda}$.

We shall refer to them as the Yukawa symmetry limits.

1. Scenario A

From Eq.(8) the charged lepton matrix in the basis $\mathcal{E} = (e_w, E_1, E_2)$ is

$$M_E \sim \frac{w}{\sqrt{2}} \begin{pmatrix} y_e r & 0 & \bar{\lambda} \\ 0 & Y r & \bar{\lambda} \\ \bar{\lambda} & \bar{\lambda} & Y r \end{pmatrix}. \quad (12)$$

In the limit $r \rightarrow 0$ and $y, \bar{\lambda}$ finite the charged lepton mass matrix has the structure

$$\begin{pmatrix} 0 & 0 & 1 \\ 0 & 0 & 1 \\ 1 & 1 & 0 \end{pmatrix}. \quad (13)$$

The spectrum consists of a massless electron and two heavy degenerate leptons with mass $\sim \bar{\lambda}w$ in this limit. Returning to Eq.(12), it can be shown that the smallest eigenvalue is given by the larger of y_e, Y . This implies that in order to get the electron mass right, $Y \simeq y_e$. Thus, without loss of generality we write the charged lepton mass matrix as

$$M_E \simeq \begin{pmatrix} m_e & 0 & \bar{\lambda}w/\sqrt{2} \\ 0 & m_e & \bar{\lambda}w/\sqrt{2} \\ \bar{\lambda}w/\sqrt{2} & \bar{\lambda}w/\sqrt{2} & m_e \end{pmatrix}, \quad (14)$$

where m_e is the physical electron mass. Moreover, the parameter Y_1 remains free.

In general, we can write the physical mass eigenstates $\mathcal{E}'_\alpha = (e, E_-, E_+)$ where $\alpha = 1, 2, 3$ is given by

$$\mathcal{E}'_i = V_{i\alpha} \mathcal{E}_\alpha, \quad (15)$$

where V is the unitary matrix that diagonalizes M_E such that $(V^A)^T \cdot M_E \cdot V^A = \text{diag}\{m_e, -(\bar{\lambda}w - m_e), \bar{\lambda}w + m_e\}$. For the simplified symmetrical case of Eq.(14), V^A can be worked out to be

$$V^A \simeq \begin{pmatrix} \frac{1}{\sqrt{2}} & \frac{1}{2} & \frac{1}{2} \\ -\frac{1}{\sqrt{2}} & \frac{1}{2} & \frac{1}{2} \\ 0 & -\frac{1}{\sqrt{2}} & \frac{1}{\sqrt{2}} \end{pmatrix}. \quad (16)$$

The neutral lepton mass matrix is

$$M_N \simeq \frac{\bar{\lambda}w}{\sqrt{2}} \begin{pmatrix} 0 & 0 & 1 \\ 0 & 0 & 1 \\ 1 & 1 & 0 \end{pmatrix}. \quad (17)$$

Note that the difference between Eqs.(11) and (14) is proportional to an identical matrix. Therefore, both the neutral and charged lepton mass matrices are diagonalized by the same rotation, Eq.(16). At tree level the spectrum consists of a massless neutrino and a Dirac neutrino of mass $\sim \bar{\lambda}w$. This can be seen by defining

$n_{\mp} = \frac{1}{\sqrt{2}}(\nu_L^w \mp N_{1L})$. In the basis (n_-, n_+, N_{2R}^c) the matrix M_N becomes

$$M_N \propto \begin{pmatrix} 0 & 0 & 0 \\ 0 & 0 & 1 \\ 0 & 1 & 0 \end{pmatrix}. \quad (18)$$

Clearly n_- is massless and the pair of Weyl neutrinos n_+, N_{2R}^c combine into a Dirac neutrino. In the case that the neutrinos receive notable quantum corrections, we denote the charged neutral mass eigenstates as (ν, N_-, N_+) with the convention $M_{N_+} > M_{N_-}$.

The Y_1 Yukawa term is relevant when considering the exotic fermion decays. In the mass basis, we have the following terms:

$$\begin{aligned} & \frac{Y_1}{2} \left\{ -\bar{e}[\Re(H_1^0) + i\gamma_5 \Im(H_1^0)]e \right. \\ & + \frac{1}{\sqrt{2}}\bar{e}[\gamma_5 \Re(H_1^0) + i\Im(H_1^0)](E_+ + E_-) \\ & + \frac{1}{2}(\bar{E}_+ + \bar{E}_-)[\Re(H_1^0) + i\gamma_5 \Im(H_1^0)](E_+ + E_-) \left. \right\} \\ & - \frac{Y_1}{2} \left[\bar{\nu} + (\bar{N}_+ + \bar{N}_-)/\sqrt{2} \right] \hat{R} e H_1^+ \\ & + \frac{Y_1}{2\sqrt{2}} \left[\bar{\nu} + (\bar{N}_+ + \bar{N}_-)/\sqrt{2} \right] \hat{R} (E_+ + E_-) H_1^+ \\ & + h.c. \end{aligned} \quad (19)$$

2. Scenario B

In this case, the SM leptons completely decouple from the exotic fermion sector. The lepton matrices now become

$$M_E \sim \frac{w}{\sqrt{2}} \begin{pmatrix} y_e r & 0 & 0 \\ 0 & Y r & \bar{\lambda} \\ 0 & \bar{\lambda} & Y r \end{pmatrix}, \quad (20)$$

and M_E can be diagonalized by the rotation matrix

$$V^B \simeq \begin{pmatrix} 1 & 0 & 0 \\ 0 & \frac{1}{\sqrt{2}} & \frac{1}{\sqrt{2}} \\ 0 & -\frac{1}{\sqrt{2}} & \frac{1}{\sqrt{2}} \end{pmatrix}. \quad (21)$$

The mass eigenstates are again denoted as (e, E_-, E_+) . For neutrinos,

$$M_N = \frac{w\lambda_3}{\sqrt{2}} \begin{pmatrix} 0 & 0 & 0 \\ 0 & 0 & 1 \\ 0 & 1 & 0 \end{pmatrix}. \quad (22)$$

Clearly, there is no mixing between the ν^w and (N_{1L}, N_{2R}^c) .

In the chiral basis, M_N is also diagonalized by V^B and the mass eigenstates are again denoted as (ν, N_-, N_+) . At tree-level N_+, N_- are degenerated. In fact, N_{1L} and N_{2R} form a Dirac fermion at tree-level, let's simply call it N , and $\hat{L}N = N_{1L}, \hat{R}N = N_{2R}$. The degeneracy will be broken by the 1-loop mass correction. However, the quantum correction is expected to be much smaller than w and taking N as a Dirac DM is a good approximation.

The Y_1 Yukawa term in the mass basis becomes

$$\frac{Y_1}{\sqrt{2}} (\bar{\nu} H_1^+ + \bar{e} H_1^0) \hat{R} (E_+ + E_-) + h.c. \quad (23)$$

The heavier of E_{\pm} and H_1 can decay via this Yukawa interaction follow by the lighter one decaying through gauge interactions.

IV. GAUGE INTERACTIONS

The covariant derivative is

$$D_{\mu} = \partial_{\mu} - i\frac{g}{2}\mathbf{W}_{\mu} \cdot \boldsymbol{\tau} - ig'YB_{\mu} - ig_l(\ell)Z_{l\mu}, \quad (24)$$

where Z_l is the gauge boson for $U(1)_l$, Y the hypercharge, and ℓ the lepton number. All the quantum numbers can be read from the tables. Other notations are standard. After the SSB of $U(1)_l$, $\langle \Phi_{1,2} \rangle = w_{1,2}$, the Z_l acquires a mass

$$\begin{aligned} M_X &= g_l \sqrt{w_1^2 + 4w_2^2} \\ &= g_l \bar{w} \\ &= 2.24g_l w \text{ for } w_1 = w_2 = w, \end{aligned} \quad (25)$$

where $\bar{w}^2 = w_1^2 + 4w_2^2$ gives the overall lepton number violating scale.

In terms of the physical gauge bosons, the gauge interaction in the weak basis is

$$\begin{aligned} & ie [\bar{e}_w \gamma^{\mu} e_w + \bar{E}_1 \gamma^{\mu} E_1 + \bar{E}_2 \gamma^{\mu} E_2] P_{\mu} \\ & - \frac{ig_2}{2c_w} [\bar{\nu}_w \gamma^{\mu} \hat{L} \nu_w + \bar{N}_1 \gamma^{\mu} \hat{L} N_1 + \bar{N}_2 \gamma^{\mu} \hat{R} N_2] Z_{\mu} \\ & - \frac{ig_2}{c_w} [\bar{e}_w \gamma^{\mu} (g_L \hat{L} + g_R \hat{R}) e_w + \bar{E}_1 \gamma^{\mu} (g_L \hat{L} + g_R \hat{R}) E_1 \\ & + \bar{E}_2 \gamma^{\mu} (g_L \hat{R} + g_R \hat{L}) E_2] Z_{\mu} \\ & - \frac{ig_2}{\sqrt{2}} [\bar{\nu}_w \gamma^{\mu} \hat{L} e_w + \bar{N}_1 \gamma^{\mu} \hat{L} E_1 + \bar{N}_2 \gamma^{\mu} \hat{R} E_2] W_{\mu}^+ + h.c. \\ & - ig_l [\bar{\nu}_w \gamma^{\mu} \hat{L} \nu_w + \bar{e}_w \gamma^{\mu} e_w - \bar{N}_1 \gamma^{\mu} \hat{L} N_1 - \bar{E}_1 \gamma^{\mu} E_1] (Z_l)_{\mu}, \end{aligned} \quad (26)$$

where P denotes the photon, $g_L = -1/2 + s_w^2$ and $g_R = s_w^2$ are the SM left-handed and right-handed Z -electron coupling, respectively. We have also assumed the kinetic mixing between $U(1)_l$ and $U(1)_Y$ is negligible.

A. SM gauge interaction

For the scenario-B, the weak basis and the mass basis are related by

$$\begin{aligned} e_w &= e, \\ E_1 &= \frac{1}{\sqrt{2}}[E_+ + E_-], \\ E_2 &= \frac{1}{\sqrt{2}}[E_+ - E_-], \end{aligned} \quad (27)$$

$$\begin{aligned} \nu_w &= \nu, \\ N_{1L} &= \hat{L}N = \frac{1}{\sqrt{2}}[N_+ + N_-], \\ N_{2R} &= \hat{R}N = \frac{1}{\sqrt{2}}[N_+^c - N_-^c]. \end{aligned} \quad (28)$$

The mass splitting between N_+ and N_- could stem from the quantum corrections and is unlikely to be experimentally detectable. Hence, it is a very good approximation to lump them into a Dirac fermion N .

The QED interaction in the mass basis remains intact,

$$ie [\bar{e}\gamma^\mu e + \bar{E}_+\gamma^\mu E_+ + \bar{E}_-\gamma^\mu E_-] P_\mu. \quad (29)$$

The SM CC interaction becomes

$$-\frac{ig_2}{\sqrt{2}} \left[\bar{\nu}\gamma^\mu \hat{L}e + \frac{1}{\sqrt{2}}\bar{N}\gamma^\mu E_+ - \frac{1}{\sqrt{2}}\bar{N}\gamma^\mu \gamma^5 E_- \right] W_\mu^+ + h.c. \quad (30)$$

The SM CC interaction is intact. However, note that the $\bar{N}E_+W^+$ vertex is vector-like and the $\bar{N}E_-W^+$ one is axial-vector.

The SM NC interaction admits a similar structure and becomes

$$\begin{aligned} &\left\{ -\frac{ig_2}{2c_w} [\bar{\nu}\gamma^\mu \hat{L}\nu + \bar{N}\gamma^\mu N] - \frac{ig_2}{c_w} [\bar{e}\gamma^\mu (g_L \hat{L} + g_R \hat{R})e] \right. \\ &- \frac{ig_2}{c_w} \frac{g_L + g_R}{2} [\bar{E}_+\gamma^\mu E_+ + \bar{E}_-\gamma^\mu E_-] \\ &\left. - \frac{ig_2}{c_w} \frac{g_R - g_L}{2} [\bar{E}_+\gamma^\mu \gamma^5 E_- + \bar{E}_-\gamma^\mu \gamma^5 E_+] \right\} \times Z_\mu. \end{aligned} \quad (31)$$

For the scenario-A,

$$\begin{aligned} e_w &= \frac{e}{\sqrt{2}} + \frac{1}{2}[E_+ + E_-], \\ E_1 &= -\frac{e}{\sqrt{2}} + \frac{1}{2}[E_+ + E_-], \\ E_2 &= \frac{1}{\sqrt{2}}[E_+ - E_-], \end{aligned} \quad (32)$$

$$\begin{aligned} \nu_L^w &= \frac{\nu}{\sqrt{2}} + \frac{1}{2}[N_+ + N_-], \\ N_{1L} &= -\frac{\nu}{\sqrt{2}} + \frac{1}{2}[N_+ + N_-], \\ N_{2R} &= \frac{1}{\sqrt{2}}[N_+^c - N_-^c]. \end{aligned} \quad (33)$$

Again, we adopt the approximation where N_+, N_- form a Dirac fermion N . The neutrinos in the interaction basis become

$$\nu_L^w \simeq \frac{1}{\sqrt{2}}(\nu + \hat{L}N), N_{1L} \simeq \frac{1}{\sqrt{2}}(-\nu + \hat{L}N), N_{2R} \simeq \hat{R}N. \quad (34)$$

And it is easy to check that the QED, SM-CC, SM-NC parts are the same as those in scenario-B.

In these two cases we discussed, the SM gauge couplings are intact. This is due to that $V_{31} = 0$ for both cases. In general, the SM Z - e - e and Z - ν - ν axial-vector part couplings can deviate from the SM prediction. However, the deviation is expected to be small which is controlled by the mixing, $\sim \mathcal{O}(m_l/v_1) < 10^{-7}$, between SM lepton and L_2 .

B. Z_l interactions

The corrections from any extra Z boson couplings to SM leptons are important for low energy high sensitivity experiments which can be done at the proposed lepton colliders such as the ILC[16] and CLIC[17]. And it is particularly true for Z_l . To facilitate such studies, we need to know the couplings of Z_l to the SM leptons which are also important for direct searches.

We begin with the couplings of charged leptons. It is easy to see from Eq.(24) and Table(1), the charged leptons $\mathcal{E} = (e_w, E_1, E_2)$ have vector couplings to Z_l in the gauge basis. We define a charged matrix $Q^\mathcal{E}$ representing this coupling by $\bar{\mathcal{E}}Q^\mathcal{E}\gamma_\mu\mathcal{E}Z_l^\mu$, where

$$Q^\mathcal{E} = \begin{pmatrix} 1 & 0 & 0 \\ 0 & -1 & 0 \\ 0 & 0 & 0 \end{pmatrix}. \quad (35)$$

In the mass basis the corresponding charge mass is given by

$$Q'^\mathcal{E} = V^\dagger Q^\mathcal{E} V, \quad (36)$$

where V is given by Eq.(15). Specific examples of V are given in Eq.(16) and Eq.(21). In general, $Q'^\mathcal{E}$ is not diagonal and in sharp contrast to case of the SM gauge interactions. Of particular interest is $Q'_{11}^\mathcal{E} = |V_{e1}|^2 - |V_{E1}|^2$ which determines the coupling strength of Z_l to the physical electrons. For scenario-A, we see that not only is this suppressed by matrix elements but an accidental cancellation also occurs. Indeed for the simplified case it vanishes as from Eq.(16).

Similarly, we find $Q'_{12}^\mathcal{E} = V_{e1}^* V_{E2} - V_{E1}^* V_{e2}$ which gives the off diagonal coupling of Z_l to the physical electron and new heavy charged lepton. Explicitly, we have for scenario-A and in Yukawa symmetry limit

$$-\frac{ig_l}{\sqrt{2}} [\bar{e}\gamma^\mu (E_+ + E_-) + (\bar{E}_+ + \bar{E}_-)\gamma^\mu e] Z_{l\mu}. \quad (37)$$

In general, the coupling $Q_{11}^{\mathcal{E}} \bar{e} \gamma_{\mu} e Z_l^{\mu}$ will not vanish since the λ 's are all different and a complete cancelation is not expected. Moreover, it is expected that $|Q^{\mathcal{E}}| < 1$.

On the other hand, it is very different for scenario-B. In this case, the SM electron decouples from the exotic fermion and one has $Q_{11}^{\mathcal{E}} = 1$. Instead we have

$$ig_l \left[\frac{1}{2} (\bar{E}_+ + \bar{E}_-) \gamma^{\mu} (E_+ + E_-) - \bar{e} \gamma^{\mu} e \right] Z_{l\mu}. \quad (38)$$

In both scenarios the couplings are vectorial.

Similar considerations for the neutral leptons give for scenario-A

$$-\frac{ig_l}{2} \left[\bar{\nu} \gamma^{\mu} \hat{L} N + \bar{N} \gamma^{\mu} \hat{L} \nu \right] Z_{l\mu}, \quad (39)$$

and for scenario-B

$$ig_l \left[\bar{N} \gamma^{\mu} \hat{L} N - \bar{\nu} \gamma^{\mu} \hat{L} \nu \right] Z_{l\mu}. \quad (40)$$

In contrast to the charged leptons, these couplings are lefthanded.

V. PHENOMENOLOGY OF Z_l

It is clear that Z_l has only tree level couplings to SM leptons and not to quarks. Hence its phenomenology is very different from most extra Z extensions of the SM.

For scenario-A in the Yukawa symmetry limit, Z_l does not couple to SM charged leptons phenomenology at tree level although 1-loop effect can exist. Thus, we do not expect such probes to be sensitive to Z_l in this limiting case. On the other hand for scenario-B, this coupling is at full strength. Therefore, in the following, we mainly focus on the Z_l phenomenology for scenario-B. In between the two cases, our results can be used by properly multiplying by the appropriate factor $(Q^{\mathcal{E}})^2$ once elements of the mixing matrix V is determined.

Although the model has many parameters, most of which are related to that many scalars present. For Z_l phenomenology they largely do not play a role. The controlling parameters are g_l and M_X , the mass of Z_l . Whether the new leptons and scalars are heavier or lighter than Z_l mainly affects the branching ratio of Z_l into SM states, and is of secondary importance here. For definiteness, we shall assume that Z_l is the lightest of the new particles.

Direct production from e^+e^- colliders via $e^+e^- \rightarrow Z_l$ which subsequently decays into $\ell^+\ell^-$ pairs gives unambiguous signal if kinematically allowed. Indirect virtual exchange of Z_l effects can be discerned in low energy precision experiments involving only leptons. Some notable reactions are studied below.

A. LEP II bound

The four-lepton contact interactions between electrons and charged leptons ℓ with scale Λ_{VV} ⁶ is parameterized by

$$\frac{4\pi}{(\Lambda_{VV})^2} (\bar{e} \gamma^{\mu} e) (\bar{l} \gamma_{\mu} l). \quad (41)$$

This can be generated by exchanging a heavy Z_l boson with the coupling g_l . Since the leptons are mass eigenstates the coupling has to be scaled by the factor $Q_{11}^{\mathcal{E}}$. The operator yields a destructive interference with the SM process for $\sqrt{s} \ll M_X$. The resulting effects to $e^+e^- \rightarrow l^+l^-$ have been searched for at LEP and a limit that $\Lambda_{VV} > 20.0$ TeV is set if the universality between leptons is assumed[18]. This amounts to a ρ -dependent lower bound on M_X ,

$$M_X \geq \sqrt{\rho} \sqrt{\alpha} \times 20.0 \text{ TeV} \sim 1.77 \sqrt{\rho} \text{ TeV}. \quad (42)$$

where $\rho \equiv (g_l/e)^2$. For example, $M_X > 0.97$ TeV if $\rho = 0.3$. The above limit works for scenario (B) where $Q_{11}^{\mathcal{E}} = 1$. On the other hand, there is no such tree-level contact interaction for scenario-A since $Q_{11}^{\mathcal{E}} = 0$ and the LEP bound does not apply at all.

For the remainder of this section, scenario (B) is assumed.

B. Z_l width

With the assumptions listed the main decay modes of Z_l are into the SM leptons. The total width can be calculated to be:

$$\Gamma_{Z_l} = \sum_l \frac{\alpha \rho}{6} M_X (1 + 2x_l) \sqrt{1 - 4x_l} [(l_L^l)^2 + (l_R^l)^2], \quad (43)$$

where $x_l = (m_l/M_X)^2$, α the fine structure constant, and the $l_{L,R}^l$ is the left/right-handed coupling for the l lepton flavor. Since $x_l \ll 1$, we have $\Gamma_{Z_l} = \frac{3}{2} \alpha \rho M_X$. For a light Z_l , $M \sim \mathcal{O}(100)$ GeV, its typical width is around a few GeV, and its decay branching ratios are $Br(Z_l \rightarrow l^+l^-) = 2/9$ and $Br(Z_l \rightarrow \nu\bar{\nu}) = 1/9$ for each flavor.

C. Front-back asymmetry (A_{FB}) in $e^+e^- \rightarrow \mu^+\mu^-$

The exchange of Z_l which has vector couplings to e, μ will interfere with the SM exchange of Z, γ . The differential cross section is given by

⁶ Note that if $l = e$ there will be an extra symmetry factor 2 in the denominator of Eq.(41).

$$\begin{aligned}
\frac{d\sigma}{d\cos\theta} = & \frac{\pi\alpha^2}{2s} \{ |D_{\gamma l}|^2 (1 + \cos^2\theta) \\
& + \frac{1}{4(s_W c_W)^4} |D_Z|^2 [(g_L^2 + g_R^2)^2 (1 + \cos^2\theta) \\
& + 2(g_L^2 - g_R^2)^2 \cos\theta] \\
& + \frac{1}{2(s_W c_W)^2} \Re(D_{\gamma l}^* D_Z) [(g_L + g_R)^2 (1 + \cos^2\theta) \\
& + 2(g_L - g_R)^2 \cos\theta] \} , \quad (44)
\end{aligned}$$

where θ is the scattering angle of μ^- , and s is the center of mass energy squared. And $c_W(s_W)$ is the cosine(sine) of the weak mixing angle. Also the SM Z-lepton couplings are $g_L = -\frac{1}{2} + s_W^2$ and $g_R = s_W^2$. We have also introduced the dimensionless gauge boson propagator factors:

$$\begin{aligned}
D_{\gamma l} &= 1 + \frac{\rho s}{s - M_X^2 + iM_X \Gamma_X} , \\
D_Z &= \frac{s}{s - M_Z^2 + iM_Z \Gamma_Z} , \quad (45)
\end{aligned}$$

where M_X the mass and Γ_X the width of Z_l . We have combined the photon and Z_l exchange together since both have vector couplings to e and μ . The finite widths are included to take care of the behaviors near the mass poles. The SM $\gamma - Z$ interference causes a wiggling with magnitude around $\sim \mathcal{O}(10^{-2})$ of the cross section around Z-pole, see Fig.1(a,b). This along with other asymmetries have been experimentally confirmed by analyzing the Z line shape[18, 19]. The presence of the new Z_l boson provide additional wiggling around the SM Z-pole at the level of $\sim \mathcal{O}(10^{-3})$, Fig.1(b). This will be the first unambiguous sign of the existing of a new gauge boson which interferes with γ, Z , which can be searched for at the future Z factories such as the FCC-ee[20] and CEPC[21].

We parameterize the cross section as

$$\frac{d\sigma}{d\cos\theta} = \frac{\pi\alpha^2}{2s} [A(1 + \cos^2\theta) + B\cos\theta] . \quad (46)$$

Then A_{FB} is given by

$$\begin{aligned}
A_{FB} &= \frac{\int_0^1 d\cos\theta \frac{d\sigma}{d\cos\theta} - \int_{-1}^0 d\cos\theta \frac{d\sigma}{d\cos\theta}}{\int_{-1}^1 d\cos\theta \frac{d\sigma}{d\cos\theta}} \\
&= \frac{3B}{8A} , \quad (47)
\end{aligned}$$

where A, B can be easily read from Eq.(44). A_{FB} is center-of-mass energy dependent.

At the Z pole, we have

$$A_{FB} = \frac{3(g_R^2 - g_L^2)^2}{4(g_R^2 + g_L^2)^2} \sim 0.01695 \quad (48)$$

by using $s_W^2 = 0.2311$. It is accidentally small because s_W^2 is very close to $1/4$. It is interesting to note that

the Z_l exchange induces a universal positive contribution to all A_{FB}^l for SM charged leptons at the Z-pole. This can be understood because as follow. Firstly, a Z_l is heavier than M_Z it gives a destructive interference to the symmetric $D_{\gamma l}$ term and reduces A . Secondly, the asymmetric $(g_L - g_R)^2 (\gg (g_L^2 - g_R^2)^2)$ term from Z_l -SM interference increases B in Eq.(47). On the other hand, the A_{FB}^q for SM quarks receive no such contributions. Therefore, with the presence of Z_l and $M_X > M_Z$, $A_{FB}^l > A_{FB}^q$ is a robust prediction. For A_{FB}^b , the LEP experimental value is measured to be 0.0992(16) and the SM expectation is 0.1031(3) [22] by using the above value of s_W and all other SM parameters input from the global Electroweak precision fit. Or roughly speaking, $A_{FB}^l/A_{FB}^q = 1.0393 \pm 0.0164$.

However, taking into account the mass bound, Eq.(42), only a 10.7 TeV Z_l with $\rho \sim 36.3$ can explain this difference between lepton and quark sector at 2σ level. In other words, with $g_l \sim 6e$ one can account for this discrepancy. Certainly, this issue will be clarified at a future Z-factory option e^+e^- colliders.

Beyond the Z-pole and for $M_Z \ll \sqrt{s} \ll M_X$,

$$\begin{aligned}
A_{FB} &\sim \frac{3}{4} \frac{(g_R^2 - g_L^2)^2 + 2(s_W c_W)^2 (g_R - g_L)^2}{4(s_W c_W)^4 + (g_R^2 + g_L^2)^2 + 2(s_W c_W)^2 (g_R + g_L)^2} \\
&\sim 0.4691 . \quad (49)
\end{aligned}$$

At the Z_l pole, the asymmetry is small due to the vector coupling nature of Z_l and it becomes

$$\begin{aligned}
A_{FB} &\sim \frac{3}{4} \frac{(g_R - g_L)^2}{(g_R + g_L)^2 + 2(s_W c_W)^2 \frac{2}{3\alpha}} \\
&\sim 8.83 \times 10^{-6} \quad (50)
\end{aligned}$$

by using Eq.(43). It is interesting that the above three values are not sensitive to ρ . Finally, for $\sqrt{s} \gg M_X$

$$\begin{aligned}
\frac{4}{3} A_{FB} &\sim \frac{(g_R^2 - g_L^2)^2 + 2\bar{\rho}(s_W c_W)^2 (g_R - g_L)^2}{4(s_W c_W)^4 \bar{\rho}^2 + (g_R^2 + g_L^2)^2 + 2\bar{\rho}(s_W c_W)^2 (g_R + g_L)^2} , \quad (51)
\end{aligned}$$

where $\bar{\rho} = 1 + \rho$. We give a plot of A_{FB} , Fig.2, for $M_X = 2$ TeV and $\rho = 0.3, 1.0$.

The \sqrt{s} dependent A_{FB} provides an important handle to probe the new heavy gauge boson. It is especially useful for the planned linear colliders. For example, the CLIC has plans for 2-staged intermedin energy at $\sqrt{s} = 0.5, 1.4(1.5)$ TeV before reaching its ultimate 3TeV goal[17]. At each new stage, it is able to tune down the energy by about factor 3 without losing the luminosity. One might be able to see the effect of new gauge boson in the A_{FB} even if Z_ℓ is too heavy to be produced on shell.

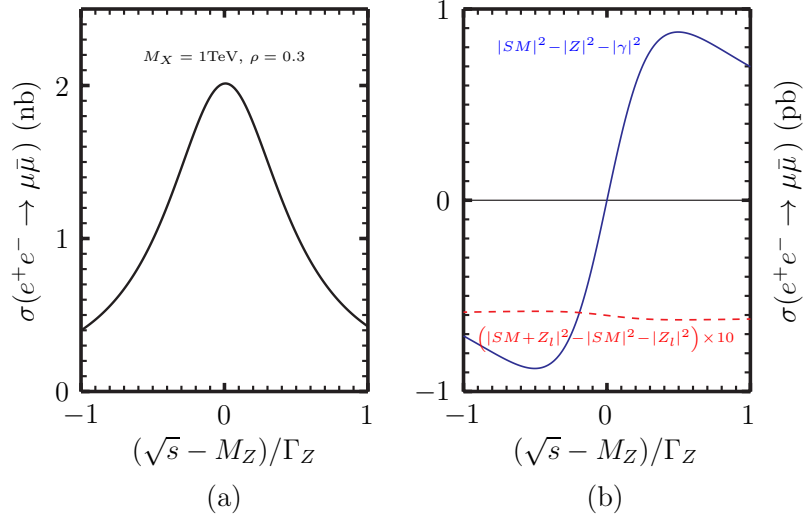


FIG. 1. (a) The line shape of $e^+e^- \rightarrow \mu\bar{\mu}$ cross section near the Z-pole for $M_X = 1\text{TeV}$ and $\rho = 0.3$. (b) The SM photon-Z interference, and the Z_l -SM interference.

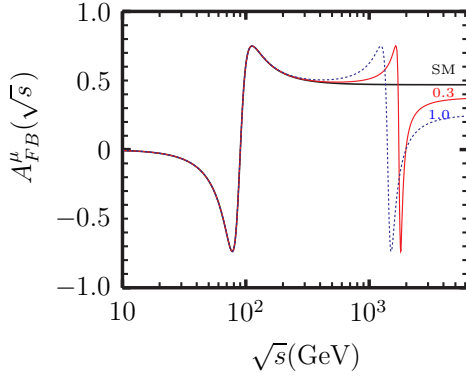


FIG. 2. The A_{FB} vs \sqrt{s} with $M_X = 2\text{TeV}$. The black curve is for the SM, and the red(blue) curve is for a Z_l with $\rho = 0.3(1.0)$.

D. Muon $g - 2$

Z_l contribution to the muon anomalous moment an amount easily calculated to be

$$\Delta a_\mu = \frac{\alpha}{3\pi} \rho \left(\frac{m_\mu^2}{M_X^2} \right). \quad (52)$$

Using the value $a_\mu^{exp} - a_\mu^{th} = 2.88 \times 10^{-9}$ [22] and requiring that Δa_μ is smaller than that, we obtain the constraint $M_X > 54.5\sqrt{\rho}$ GeV. The helicity flip factor severely curtails the sensitivity of a_μ to M . The new exotic scalars have contributions to Δa_μ as well. Since their masses have to be heavier than $\sim 0.8\text{TeV}$, those contributions are negligible. However, this limit can not compete with Eq.(42).

E. Møller Scattering

The exchange of Z_l will interfere with the SM Z, γ processes at the amplitude level. The leading order is free of hadronic uncertainties and hence offers a very clean sensitive probe of Z_l . Since the Z_l admits vector-coupling to the electron, it does not contribute left-right asymmetry directly. Its role in the Møller scattering is to increase the symmetric cross section from the photon exchange diagram. The asymmetry is then reduced to

$$A_{LR} \simeq A_{LR}^{SM} \times \left[1 - 6 \frac{\rho Q^2}{M_X^2} \frac{(1-y)(1+y+y^2)}{1+y^4+(1-y)^4} \right], \quad (53)$$

$$A_{LR}^{SM} = \frac{4G_\mu s}{\sqrt{2}\pi\alpha} \frac{y(1-y)}{1+y^4+(1-y)^4} \left[\frac{1}{4} - s_w^2 \right], \quad (54)$$

where $y = -\frac{t}{s}$. The asymmetry was measured to be

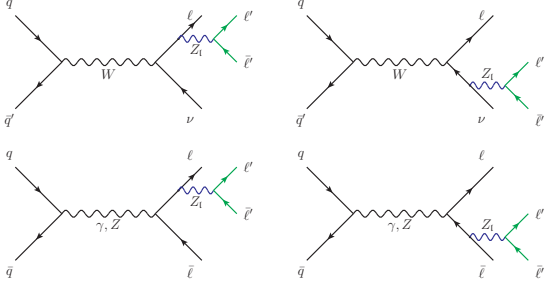
$$A_{LR} = 131 \pm 14(\text{stat}) \pm 10(\text{syst})\text{ppb} \quad (55)$$

by the SLAC E158 experiment [23], where $Q^2 = 0.026(\text{GeV})^2$, $y = 0.6$, thus $A_{LR}^{SM} = 1.47 \times 10^{-7}$. By taking 95%CL limit, $-0.337 < \frac{\delta A_{LR}}{A_{LR}} < 0.122$. Due to the stringent limits from Eq.(42), the Z_l contribution to $\frac{\delta A_{LR}}{A_{LR}}$ has no significance at all.

F. Z_l production at the LHC

If energetically allowed, Z_l can be produced at the LHC via the radiative Drell-Yan process as depicted in Fig.(3).

The final states will be 2 pairs of leptons with different flavors in which one pair constitutes a resonance. E.g. $\mu^+\mu^-$ and e^+e^- pairs and either pair coming from on-shell Z_l decay. Another signal will be three leptons plus missing energy. A spectacular example will be a $\mu^+\mu^-$

FIG. 3. Drell-Yan production of Z_l .

and an e^+e^- pair with either one pair resulting from Z_l decay. Both signatures will have no jet activities.

Here, just for illustration purpose, we consider the signal $pp \rightarrow e^+e^-Z_l \rightarrow e^+e^- + (\mu\bar{\mu})$ and there is a sharp resonance peak of muon pair invariant mass at M_X . The SM background is $pp \rightarrow e^+e^-\mu^+\mu^-$ with the $m_{\mu\bar{\mu}} \sim M_X$. We evaluate the cross section of $pp \rightarrow e^+e^-Z_l$ at LHC for three CM energies by the program CalcHep[24] with the CTEQ611 PDF set[25]. The SMBG are also evaluated by CalcHep with a cut that $m_{\mu\bar{\mu}} \in (M_X - 50\text{GeV}, M_X + 50\text{GeV})$. The numbers are listed in Tab.III.

$\frac{\sqrt{s}}{\text{TeV}}$		$\frac{M_X}{\text{TeV}} = 0.5$	$\frac{M_X}{\text{TeV}} = 1.0$	$\frac{M_X}{\text{TeV}} = 2.0$	$\frac{M_X}{\text{TeV}} = 5.0$
14	$\frac{\sigma}{g_l^2}$	5.4×10^{-5}	1.7×10^{-6}	1.9×10^{-8}	9.8×10^{-13}
	σ_{BG}	2.2×10^{-5}	1.4×10^{-6}	5.4×10^{-8}	6.2×10^{-11}
	$\frac{\bar{w}_{max}}{\text{TeV}}$	0.61	0.43	-	-
30	$\frac{\sigma}{g_l^2}$	2.6×10^{-4}	1.5×10^{-5}	5.1×10^{-7}	1.0×10^{-9}
	σ_{BG}	6.8×10^{-5}	7.1×10^{-6}	4.2×10^{-7}	5.7×10^{-9}
	$\frac{\bar{w}_{max}}{\text{TeV}}$	1.02	0.85	-	-
100	$\frac{\sigma}{g_l^2}$	1.7×10^{-3}	1.5×10^{-4}	1.1×10^{-5}	1.8×10^{-7}
	σ_{BG}	3.0×10^{-4}	3.2×10^{-5}	2.8×10^{-6}	7.6×10^{-8}
	$\frac{\bar{w}_{max}}{\text{TeV}}$	1.79	1.85	1.83	-

TABLE III. The $pp \rightarrow e^+e^-Z_l$ cross section normalized by g_l^2 and the SM BG. The cross sections are in (pb) , and \bar{w}_{max} are in TeV.

We use $S/\sqrt{B} = 3$ and an integrated luminosity $\mathcal{L}_0 = 3000(fb)^{-1}$ as the bench mark limit of detecting a Z_l at the LHC. Then

$$3 = \frac{\sigma(pp \rightarrow e^+e^-Z_l(\mu\bar{\mu}))Br(Z_l \rightarrow \mu\bar{\mu}) \times \mathcal{L}_0}{\sqrt{\sigma_{BG} \times \mathcal{L}_0}} \quad (56)$$

$$= \frac{2}{9} \sqrt{\frac{\mathcal{L}_0}{\sigma_{BG}}} \left(\frac{\sigma}{g_l^2} \right) g_l^2.$$

The corresponding highest lepton number breaking

scale we can probe is $\bar{w}_{max}^2 = (2/27)\sqrt{\mathcal{L}_0/\sigma_{BG}} \times (\sigma/g_l^2)M_X^2$, which are also displayed in Tab.III. The LHC14, LHC30, and LHC100 have the potential to probe the lepton number violating scales up to $\sim 0.5, 1.0$, and 2.0 TeV, respectively.

VI. RADIATIVE SEESAW MASS FOR ν_L

The Feynman diagrams for radiative ν_L mass generation are depicted in Fig.4 which are given in the weak eigenbasis. They fill in the upper left-hand block of zeros in Eq.(18)⁷.

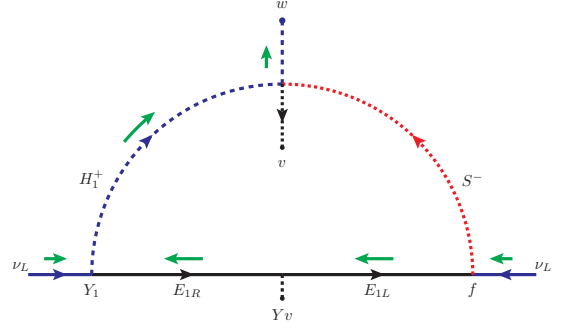


FIG. 4. 1-loop $\nu_e \nu_e$ mass term generation. Green arrows show the flow of lepton charge

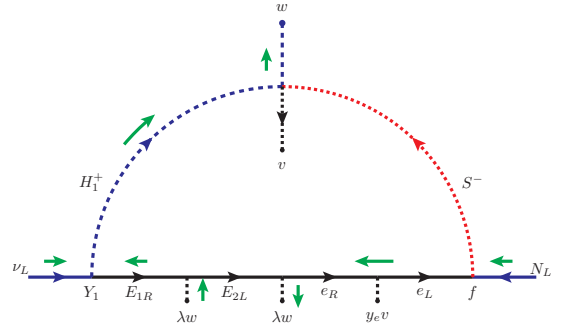


FIG. 5. 1-loop $\nu_{eL} N$ mass term generations. Green arrows show the flow of lepton charge.

In the limit that the charged H_1, S scalars are heavier than the leptons we get

$$M_{11} = \frac{f(Y_1 v)(\lambda_{1\ell} w)m_e}{16\pi^2(m_1^2 - m_S^2)} \ln \left(\frac{m_1^2}{m_S^2} \right), \quad (57)$$

where we have used $Yv = m_e$ as explained above. M_{11} will be the upper leftmost entry in Eq.(18). Similarly, we

⁷ Our anomaly solutions can accommodate a variant of the type I seesaw mechanism by adding a set of vectorlike SM singlet neutrinos \mathcal{N}_R and \mathcal{N}_L with lepton number unity. We shall not pursue this further.

get radiative correction to $M_{12,21}$, Fig.5. Clearly, these are much smaller than $\bar{\lambda}w$. Other than providing a Majorana mass for the active neutrino ν_e , they also transform the Dirac neutrino N into a pseudo-Dirac one. Numerically, the splitting will be undetectably small that for all practical purposes, and we can treat the N as a Dirac neutrino. Assuming that there is no outstanding hierarchy between m_1 and m_S , then one expects the combination $w/(m_1^2 - m_S^2) \ln(m_1^2/m_S^2) \simeq w \sim \mathcal{O}(\text{TeV})$. Plugging in the values, the resulting active neutrino mass is around $m_\nu \sim fY_1\lambda_{1\ell} \times 10^3 \text{ eV}$. And the sub-eV neutrino mass can be easily achieved with $f, Y_1, \lambda_{1\ell} \sim \mathcal{O}(0.1)$ without prominent fine tuning.

VII. PHENOMENOLOGY OF E, N

Even if the exotic leptons are too heavy to be produced by current or near future colliders they can have important effects at current energies. The notable ones are the electroweak oblique parameters S, T [26, 27], and the decay $h \rightarrow \gamma\gamma$.

A. Oblique parameters S, T

It is well known that the oblique parameters S and T constraint heavy fermions that carry SM quantum numbers. In this case they constrain the mass differences of the lepton pairs E, N as well as the number of such pairs. Explicitly, for each generation we have

$$\Delta T = \frac{1}{16\pi s_w^2} \sum_{i=1,2} \frac{M_{E_i}^2}{M_W^2} \left(1 + x_i + \frac{2x_i}{1-x_i} \ln x_i \right), \quad (58)$$

$$\Delta S = \frac{1}{6\pi} \sum_{i=1,2} (1 + \ln x_i), \quad (59)$$

where $x_i = M_{N_i}^2/M_{E_i}^2$. When the mass splitting between E_i and N_i is small comparing to their masses,

$$\begin{aligned} \Delta T &\sim \frac{1}{12\pi s_w^2 M_W^2} [(M_{N_1} - M_{E_1})^2 + (M_{N_2} - M_{E_2})^2], \\ \Delta S &\sim \frac{1}{3\pi} \left[1 + \frac{M_{N_1} - M_{E_1}}{M_{E_1}} + \frac{M_{N_2} - M_{E_2}}{M_{E_2}} \right], \end{aligned} \quad (60)$$

for each generation. The doublet H_1 provides contribution

$$\Delta T = \frac{1}{16\pi s_w^2} \frac{M_{H^+}^2}{M_W^2} \frac{1}{z} \left[1 + z + \frac{2z}{1-z} \ln z \right], \quad (61)$$

$$\Delta S = -\frac{1}{12\pi} \ln z, \quad (62)$$

where $z \equiv M_{H^+}^2/M_{H_0^0}^2$. Note that ΔT from fermions and doublet scalar are both positive, but ΔS from the doublet scalar can be either positive or negative. From the Particle Data Group, we have $S_{data} < 0.22$ and $T_{data} < 0.27$ at 95% C.L.[22]

To see how these will restrict the parameters of our model, we begin by taking $z = 1$, i.e. the neutral and charged components of H_1 are degenerate. This implies that the mixing of H_1 with all other scalars are negligible. Then the scalar contributions to ΔT and ΔS are vanishing. For simplicity we also assume the masses of E_+ and E_- are equal and their counterparts for μ and τ families are also the same. From Eq.(59) we see that the new isodoublet chiral leptons cannot have degenerate upper and lower components; otherwise it runs afoul of S_{data} . The splitting between the neutral and charged components that saturates T_{data} is given by

$$x = 0.73 \quad (63)$$

where we have dropped the subscript i . Using Eq.(58) and T_{data} we obtain $M_E \leq 350 \text{ GeV}$. The above values are to be taking as a demonstration that the stringent constraints of oblique corrections can be satisfied with new lepton masses in the range of 350 GeV, the vertical dash blue line in Fig.6. This is well above limit form the charged lepton searches of $> 100.8 \text{ GeV}$, the vertical dash red line in Fig.6, given in PDG[22]⁸.

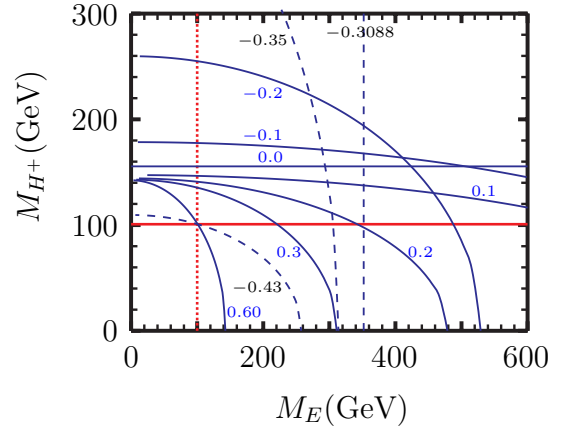


FIG. 6. Contours from ΔS and ΔT constraints for different $\ln x$. For a given $\ln x$, the allowed masses region is above the direct search bound on M_{H^+} , the horizontal red line, to the right of the direct search bound on M_E , the vertical dashed red line, and to the lower left of the blue (dash)curve.

We can also take the limit that the E and N are degenerate, i.e. all $x = 1$. Then Eq.(59) yields $\Delta S \simeq .32$. Then it will require H_1 doublet with $\ln z \simeq 3.71$ to bring it within the experimental bound since scalars give a negative contribution (see Eq.(62)). The scalars will then be the sole contributors to ΔT . A similar calculation gives an upper on the mass of H^+ to be 155 GeV, the horizontal blue line in Fig.6. This value is also larger than the direct

⁸ Note that the limit, $M_E \gtrsim 168 \text{ GeV}$ at 95% C.L., obtained by [28] does not apply here since there is no tree-level Z - E - l coupling in our model.

search bound on charged scalars, the horizontal red line in Fig.6. The large splitting between H^+ and H_1^0 implies that some if not all of the parameters $\kappa_{H_1 S}$, $\kappa_{\Phi_i H_1}$ and μ_3 in Eq.(9) are large.

Notice that since z is large we have $M_{H_1^0} \simeq 24.4$ GeV. In general it can mix with the SM Higgs boson but we have seen that this mixing is constrained to be small. In the interaction basis, which is good for small mixings, it does not couple to quarks and it has no couplings to gluons to 1-loop. Because of this, it will not run into problem at the LHC. Neutral scalars in the mass range of 10 – 100 GeV is notoriously difficult to detect. The challenges and a possible signal for probing this at the LHC was discussed in [29]. Additionally, a more promising avenue of exploring this at a future e^+e^- collider is given in [30].

From the above limiting case, it is easy to see that if $\ln x > -0.3088$ the doublet H_1 will have to play a role in satisfying the oblique corrections bounds. For $\ln x = -0.3088$, it is the vertical dashed blue line in Fig.6. It is more realistic to assume finite mass splittings between isodoublet for both leptons and scalars. As an illustration we take $\ln x = -0.2$, then the masses of M_E and M_{H^+} will satisfy a contour given by

$$.0062 \left(\frac{M_E}{M_W} \right)^2 + .0259 \left(\frac{M_{H^+}}{M_W} \right)^2 \leq 0.27. \quad (64)$$

The allowed regions of M_E and M_{H^+} for different $\ln x$ are displayed in Fig.6. If both experimental lower bounds on M_E , M_{H^+} are met, one can see that the range of $\ln x$ is $-0.43572 < \ln x < 0.6053$, and it implies that $0.80 < (M_N/M_E) < 1.35$ and $0.47 < (M_{H^+}/M_{H^0}) < 241.0$ if a universal x_i is assumed. Moreover, for $\ln x > -0.1$, a light neutral scalar with mass $M_{H^0} < 50$ GeV is expected.

Before closing this section, we remark that it is well-known that the constraint from ΔT can be largely loosen by introducing an $SU(2)$ triplet with a small VEV so that the tree-level electroweak ρ -parameter is less than unity. However, for the minimal setup, we do not further into such discussion.

B. Impact on Higgs decays

1. Higgs to two photons.

The SM Higgs to the di-photon vertex is generated at the 1-loop level with dominant contributions from W^\pm and top quark running in the loop. In our model, there are six new charged leptons, a E_1, E_2 pair for each of the three generations, and two new charged scalars, H_1^\pm and S^\pm . These charged fields mix among themselves, and one needs to know every parameter for the actual mass diagonalization. However, with assumptions on the mass ranges of these charged particles, a general discussion is sufficient to draw qualitative conclusions.

In the mass basis, we can parameterize the Yukawa couplings and cubic couplings to the SM Higgs as

$$\mathcal{L} \supset - \sum_{i=1}^6 y_{E_i} \bar{E}_i E_i h - \sum_{i=1,2} \lambda_i M_W h H_i^+ H_i^-. \quad (65)$$

These new electrically charged degrees of freedom enter the 1-loop triangle diagram and modify the width of the SM Higgs di-photon decay. This is given by [31]

$$\Gamma(H \rightarrow \gamma\gamma) = \frac{G_F \alpha^2 M_H^3}{128 \sqrt{2} \pi^3} \left| F_1(\tau_W) + \frac{4}{3} F_{1/2}(\tau_t) + \sum_{j=1,2} \lambda_j \frac{M_W^2}{g_2 M_{H_j}^2} F_0(\tau_{H_j}) + \sum_{i=1}^6 y_{E_i} \frac{2M_W}{g_2 M_{E_i}} F_{1/2}(\tau_{E_i}) \right|^2, \quad (66)$$

where $\tau_i \equiv (m_H/2m_i)^2$, and

$$\begin{aligned} F_0(\tau) &= -[\tau - f(\tau)]/\tau^2, \\ F_{1/2}(\tau) &= 2[\tau + (\tau - 1)f(\tau)]/\tau^2, \\ F_1(\tau) &= -[2\tau^2 + 3\tau + 3(2\tau - 1)f(\tau)]/\tau^2, \end{aligned} \quad (67)$$

with

$$f(\tau) = \begin{cases} [\sin^{-1} \sqrt{\tau}]^2, & \text{if } \tau \leq 1 \\ -\frac{1}{4} \left[\log \frac{1+\sqrt{1-1/\tau}}{1-\sqrt{1-1/\tau}} - i\pi \right]^2, & \text{if } \tau > 1. \end{cases} \quad (68)$$

For $m_i \gg M_H/2 = 62.5$ GeV, we have the following expansions around $\tau = 0$:

$$\begin{aligned} F_0(\tau) &\sim \frac{1}{3} + \frac{8}{45}\tau + \mathcal{O}(\tau^2), \\ F_{1/2}(\tau) &\sim \frac{4}{3} + \frac{14}{45}\tau + \mathcal{O}(\tau^2), \\ F_1(\tau) &\sim -7 - \frac{22}{15}\tau + \mathcal{O}(\tau^2). \end{aligned} \quad (69)$$

Plugging in the numbers, the di-photon decay width reads

$$\begin{aligned} \Gamma(H \rightarrow \gamma\gamma) &= \frac{G_F \alpha^2 M_H^3}{128 \sqrt{2} \pi^3} \times \left| -8.324 + 1.834 \right. \\ &\quad \left. + 8.3 \times 10^{-4} (1.3 \times 10^{-2}) \times \lambda_2 + 0.087(0.42) \times \lambda_1 \right. \\ &\quad \left. + \sum_{i=1}^6 0.32(3.64) \times y_{E_i} \right|^2 \end{aligned} \quad (70)$$

for $M_{E_i} = 1000(100)$ GeV, $M_{H_2} = 2.0(0.5)$ TeV, and $M_{H_1} = 200(100)$ GeV. The first two numbers are the dominate SM contributions from W^\pm and top quark, respectively. Since we expect $|y_{E_i}| \sim m_l/v_h \ll 1$, even for the new leptons (see Sec. III) the charged leptons contribution can be ignored. If the second charged scalar is heavy, its contribution can be ignored too even taking $\lambda_2 \sim \mathcal{O}(1)$. Therefore, only the light charged scalar with

mass in the range of 100 to 200 GeV matters. The gluon fusion is the dominant SM Higgs production channel at the LHC, and it does not receive any modification. The signal strength of $pp \rightarrow h \rightarrow \gamma\gamma$ at the LHC is therefore

$$\begin{aligned}\mu_{\gamma\gamma} &\simeq \Gamma(H \rightarrow \gamma\gamma)/\Gamma(H \rightarrow \gamma\gamma)_{SM} \\ &\sim 1 - (0.03 - 0.13) \times \lambda_1.\end{aligned}\quad (71)$$

Comparing with the experiment data $\mu_{\gamma\gamma} = 1.18(+0.17 - 0.14)$ [32], we conclude that it is safe even the light charged Higgs has a coupling $|\lambda_1| \sim \mathcal{O}(1)$. This is in agreement with the general analysis given in [33].

2. Higgs to 4 fermions

For notational simplicity, here we denote $h_1 \equiv \Re(H_1^0)$ and $a_1 \equiv \Im(H_1^0)$. If h_1 (or a_1) is lighter than half the mass of the SM Higgs, h_{SM} , then we can have

$$h_{SM} \rightarrow 2h_1(2a_1) \rightarrow \bar{\ell}_i \ell_i + \bar{\ell}_j \ell_j. \quad (72)$$

The decay width is

$$\Gamma(h_{SM} \rightarrow h_1 h_1(a_1 a_1)) = \frac{v^2(\kappa_2 + \kappa_3)^2}{32\pi M_H} \left(1 - \frac{4m_1^2}{M_H^2}\right)^{\frac{1}{2}} \quad (73)$$

where $M_H (= 125\text{GeV})$ and m_1 are the masses of h_{SM} and $h_1(a_1)$ respectively. We have neglected term involving off diagonal mixing of neutral scalars. The dominant decay mode for $h_1(a_1)$ is model dependent. The current bound on the mixing squared between h_{SM} and h_1 is about $\lesssim 10^{-2}$ for $10 < m_1 < 40$ GeV from LEP2[34]⁹. For $Y_1 \sim \mathcal{O}(0.1)$, as expected from the radiative neutrino masses, the effects from the mixing with SM Higgs can not compete with those from the direct Yukawa interaction, Eq.(19). Therefore, for scenario A, the main decay channel will be $h_1(a_1) \rightarrow \bar{\ell}\ell$ with $\ell = e, \mu, \tau$. The signal will be SM Higgs decays into 2 charged leptons pairs with both invariant masses peaking at the unknown m_1 .

For scenario B, $h_1(a_1)$ has only off-diagonal couplings to SM lepton and a heavy lepton, see Eq.(23). The dominant decay of light $h_1(a_1)$ is expected to be due to mixing with the $h_{SM}(\Im(H_0^0))$ which then decays into a fermion pair. Therefore, $b\bar{b}$ will be the dominate final state if $m_1 > 10$ GeV.

For the general case, in between scenario A and B, we expect the mixing element $|U_{12}|^2 < 0.13$, from unitarity and $|U_{11}|^2 > 0.87$ [15], to be small but non-vanishing.

C. Colliders production and decay of exotic leptons

For both scenarios (A) and (B), the SM gauge interaction allows $E_{\pm} \rightarrow W^{\pm} N_{\pm}, W^{\pm} N_{\mp}$, and $N_{+} \rightarrow N_{-} Z$

if that $M_N < M_E$ is assumed. We consider the decay, $E_{\pm} \rightarrow NW^{\pm}$, of a heavy Dirac N for simplicity. The decay width is calculated to be

$$\begin{aligned}\Gamma_{E_{\pm} \rightarrow NW^{\pm}} &= \frac{G_F M_E^3}{8\sqrt{2}\pi} \lambda_{cm}(x_N, x_w) f(x_w, x_N) \\ f(x, y) &= x(1 + y - 2x \mp 6\sqrt{x}) + (1 - y)^2\end{aligned}\quad (74)$$

where $\lambda_{cm}(y, z) = \sqrt{1 + y^2 + z^2 - 2(y + z + yz)}$, $x_w = (M_W/M_E)^2$, and $x_N \equiv (M_N/M_E)^2$. For $M_E \gg M_W$, or $x_w \ll 1$, the width becomes

$$\Gamma_{E_{\pm} \rightarrow NW^{\pm}} \simeq \frac{G_F M_E^3}{8\sqrt{2}\pi} (1 - x_N)^3. \quad (75)$$

As discussed in Sec.VII A, the oblique corrections requires that $\ln x_N > -0.4357$, and results in an upper bound

$$\Gamma_{E_{\pm} \rightarrow NW^{\pm}} < 14.45 \times \left(\frac{M_E}{1\text{TeV}}\right)^3 \text{ GeV}. \quad (76)$$

On the other hand, if $M_N > M_E$, the decay width of N takes a similar form with $M_E \leftrightarrow M_N$,

$$\Gamma_{N \rightarrow E_{\pm} W^{\pm}} \simeq \frac{G_F M_N^3}{8\sqrt{2}\pi} (1 - x_N^{-1})^3. \quad (77)$$

Similarly, from that $\ln x_N < 0.6053$,

$$\Gamma_{N \rightarrow E_{\pm} W^{\pm}} < 30.72 \times \left(\frac{M_N}{1\text{TeV}}\right)^3 \text{ GeV}. \quad (78)$$

From the above discussion, unless the leptons are nearly degenerate, the decays of E_{\pm} or N are expected to be prompt.

Next, we turn our attention to the heavy lepton decay via the Yukawa interaction with H_1 . Let's consider a general case with two fermions F, f , and a scalar ϕ . The scalar field ϕ could be either neutral or charged. Assume that they admit a Yukawa interaction which is parameterized as $\mathcal{L} \supset \bar{F}(s + a\gamma^5)f\phi + h.c.$. If kinematics allowed, the decay channel $F \rightarrow f\phi$ opens and the width is calculated to be

$$\begin{aligned}\frac{\lambda_{cm}(x_f, x_{\phi})M}{16\pi} &[(1 + x_f)^2 |s|^2 \\ &+ (1 - x_f)^2 |a|^2 - x_{\phi}(|s|^2 + |a|^2)]\end{aligned}, \quad (79)$$

where M is the mass of F , $x_f = (m_f/M)^2$, and $x_{\phi} = (m_{\phi}/M)^2$. For the cases that $M, m_f \gg m_{\phi}$, the decay width becomes

$$\Gamma(F \rightarrow f\phi) \simeq \frac{M}{16\pi} (1 - x_f) [(1 + x_f)^2 |s|^2 + (1 - x_f)^2 |a|^2]. \quad (80)$$

The relevant fields and Yukawa couplings in our model are collected and listed in Tab.IV. One can read the precise expression by using Eq.(80) and Tab.IV. Roughly speaking, the decay widths are about $\sim (Y_1^2/64\pi)M$, or numerically $\sim 0.05 \times (Y_1/0.1)^2 \times (M/1\text{TeV}) \text{ GeV}$, where

⁹ The limit on the mixing squared between h_{SM} and h_1 could be improved by a few orders of magnitude at the future colliders[29, 30].

scenario	F	f	ϕ	s	a
(A)	E_{\pm}	e	h_1	0	$-\frac{Y_1}{2\sqrt{2}}$
	E_{\pm}	e	a_1	$-\frac{iY_1}{2\sqrt{2}}$	0
	E_{\pm}	ν	H_1^-	$\frac{Y_1}{4\sqrt{2}}$	$-\frac{Y_1}{4\sqrt{2}}$
	N	e	H_1^+	$-\frac{Y_1}{4}$	$-\frac{Y_1}{4}$
(B)	E_{\pm}	e	h_1	$\frac{Y_1}{4}$	$-\frac{Y_1}{4}$
	E_{\pm}	e	a_1	$-\frac{iY_1}{4}$	$\frac{iY_1}{4}$
	E_{\pm}	ν	H_1^-	$\frac{Y_1}{2\sqrt{2}}$	$-\frac{Y_1}{2\sqrt{2}}$

TABLE IV. The H_1 Yukawa couplings between the heavy leptons and the SM ones in our model. The heavy neutrino is assumed to be Dirac.

M is the mass of E_{\pm} or N . In general, this decay width is much smaller than that from the decay with a SM W^{\pm} boson in the final states. Note that in scenario-B, N does not have the tree-level 2-body decays via the Yukawa interaction with H_1 ¹⁰. However, if the mass of the charged scalar S^{\pm} is less than M_N then the decay $N \rightarrow e^+ S^{-11}$ is possible. Otherwise N will have only 3-body decays. For $M_N < M_E$, there is another chain with an intermediate virtual E ; for example, $N \rightarrow W^+ E^* \rightarrow W^+ h_1 e^-$. We shall use the superscript “*” to denote off-shell particles.

The heavy leptons can be pair produced at the e^+e^- colliders. For simplicity, we assume that E_+ and E_- are nearly degenerate, so that they are hard to be distinguished experimentally and we collectively denote the states as $E \equiv E_+ \sim E_-$. For $\sqrt{s} \gg M_Z$ and away from the Z_{ℓ} pole, the production cross section per generation for scenario-(B) can be calculated to be

$$\begin{aligned} \sigma(e^+e^- \rightarrow E\bar{E}) \simeq & 2 \frac{4\pi\alpha^2}{3s} \sqrt{1-4x_E} \left\{ \left(1 + \frac{\rho s}{s - M_X^2} \right)^2 (1 + 2x_E) \right. \\ & + \frac{(g_L^e)^2 + (g_R^e)^2}{4(s_W c_W)^4} [(1 - x_E)((g_L^E)^2 + (g_R^E)^2) + 6x_E g_L^E g_R^E] \\ & \left. + \frac{(g_L^e + g_R^e)(g_L^E + g_R^E)}{2(s_W c_W)^2} \left(1 + \frac{\rho s}{s - M_X^2} \right) (1 - x_E) \right\} \quad (81) \end{aligned}$$

where $x_E \equiv M_E^2/s$, $g_L^E \simeq g_L^e = -1/2 + s_W^2$, $g_R^E \simeq g_R^e = s_W^2$. The first factor 2 represents the incoherent sum from the contribution of the two heavy Dirac charged leptons. For example, if $\{M_{E_+}, M_{E_-}\} = \{200, 180\}$ GeV, $\rho = 0.3$, and $M_X = 1$ TeV, the production cross section of 2 charged leptons are 556.0(83.2) fb for $\sqrt{s} = 1.2(2.2)$ TeV,

see Fig.7(a). Similarly, the heavy N can be pair produced through the s-channel process mediated by Z, Z_{ℓ} , and the production cross section for each generation is

$$\begin{aligned} \sigma(e^+e^- \rightarrow N\bar{N}) \simeq & \frac{4\pi\alpha^2}{3s} \sqrt{1-4x_N} \left\{ \left(\frac{\rho s}{s - M_X^2} \right)^2 (1 + 2x_N) \right. \\ & + \frac{(g_L^e)^2 + (g_R^e)^2}{8(s_W c_W)^4} (1 + 2x_N) \\ & \left. + \frac{(g_L^e + g_R^e)(g_L^e - g_R^e)}{2(s_W c_W)^2} \left(\frac{\rho s}{s - M_X^2} \right) (1 - x_N) \right\} \quad (82) \end{aligned}$$

For example, if $M_N = 170$ GeV, $\rho = 0.3$, and $M_X = 1$ TeV, the production cross section of $N\bar{N}$ pair are 94.0(12.4) fb for $\sqrt{s} = 1.2(2.2)$ TeV, see Fig.7(b).

At the LHC, the heavy leptons can be produced via the photon and(or) W/Z-boson Drell-Yan process. Therefore, the production cross sections are independent of the Z_{ℓ} mass and the $U(1)_{\ell}$ gauge couplings. Since a full-fledged collider study is beyond the scope of this paper, only the production cross-section are considered here. Three sets of (M_{E_+}, M_{E_-}) are considered as the benchmarks with the assumption that their mass differences are sub-electroweak. When choosing the heavy Dirac neutrino masses, the constraint from the electroweak precision have been taken into account; with $|\ln x| < \{0.3, 0.15, 0.05\}$ for $M_{E_+} = \{200, 500, 1000\}$ GeV, respectively. The production cross sections are evaluated by CalcHep and listed in TableV and TableVI.

For $M_E, M_N \lesssim 500$ GeV, the production cross sections are about $\mathcal{O}(1-100)$ fb. The production of E and N will be followed by their decays into SM particles. The decay modes are sensitive to the masses of E_{\pm}, E_{\pm}, N as well as the masses of the charged scalars H_1^{\pm}, S^{\pm} which in general mix. If the splitting between E, N is large enough the dominant decays will be 2-body modes; otherwise they will be 3-body modes. They also depend on the ordering of the E, N masses. If $M_E > M_{S^{\pm}}$ then we have the chain

$$E \rightarrow \bar{\nu} + S^- \rightarrow W^- + h_1(a_1), \quad (83)$$

where the decay of S^- proceeds via mixing with H_1^- . Additionally, in scenario-(B), if $M_E > M_N$ we also have the chain

$$\begin{aligned} E & \rightarrow W^- + N \\ & \downarrow \\ & W^- + E^{(*)} + W^+ \\ & \rightarrow e^- + h_1(a_1), \end{aligned} \quad (84)$$

where we take the decay of E to proceed via

$$E \rightarrow e + h_1(a_1) \rightarrow e + \ell\bar{\ell} \quad (85)$$

if Y_1 is not too small.

¹⁰ We have checked that even $M_N < M_E$ N can not be a dark matter candidate due to its SM $SU(2)$ interaction. Adding an ad hoc Z_2 parity will not change this.

¹¹ Due to the radiative generated Majorana masses, Fig.5, N is in fact pseudo-Dirac. However, the conjugate decays, $N \rightarrow W^- \bar{E}$ and $N \rightarrow e^- S^+$, are expected to be rare.

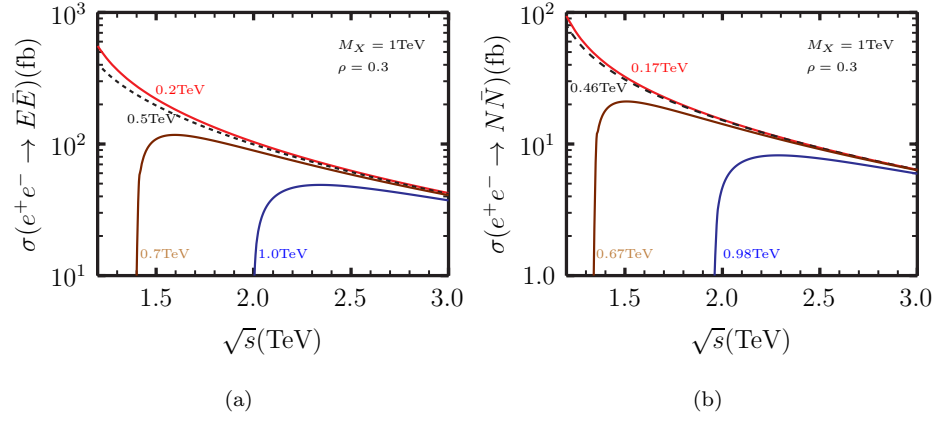


FIG. 7. (a) The $E\bar{E}$, and (b) $N\bar{N}$ production cross sections v.s \sqrt{s} at an e^+e^- collider. The masses of $E(N)$ are labeled next to the curves.

	M_{E+}	M_{E-}	\bar{E}_+E_+	$\bar{E}_+E_- + \bar{E}_-E_+$	\bar{E}_-E_-
set-1	200	180	9.62×10^{-2}	4.27×10^{-2}	1.40×10^{-1}
set-2	500	480	2.76×10^{-3}	9.04×10^{-4}	3.30×10^{-3}
set-3	1000	950	9.08×10^{-5}	2.44×10^{-5}	1.21×10^{-4}

TABLE V. The production cross sections(in pb) at the LHC14 for one generation in scenario-B in our model. The masses of E_{\pm} are in the unit of GeV.

	M_N	$\bar{N}N$	$\bar{N}E_+ + \bar{E}_+N$	$\bar{N}E_- + \bar{E}_-N$
set-1	170	3.68×10^{-1}	1.19×10^{-1}	5.20×10^{-2}
set-1	230	1.21×10^{-1}	6.90×10^{-2}	2.89×10^{-2}
set-2	460	7.76×10^{-3}	3.04×10^{-3}	1.04×10^{-3}
set-2	540	3.87×10^{-3}	2.17×10^{-3}	7.24×10^{-4}
set-3	980	1.93×10^{-4}	9.28×10^{-5}	2.69×10^{-5}
set-3	1020	1.53×10^{-4}	8.29×10^{-5}	2.37×10^{-5}

TABLE VI. The production cross sections(in pb) at the LHC14 for one generation in scenario-B in our model. The masses of N are in the unit of GeV.

Next, we examine the decays of the neutral lepton N . If $M_N > M_E$, the decay chain will be

$$N \rightarrow W^+ + E \rightarrow e^- + h_1(a_1). \quad (86)$$

Similar to the case of E , if $M_N > M_{S\pm}$ the following is also available

$$N \rightarrow e^+ + S^- \rightarrow W^- h_1(a_1). \quad (87)$$

Before one can draw any conclusion, it is crucially important to understand the SM background first. We leave the comprehensive signal and background study to a future work.

VIII. CONCLUSIONS

An anomaly free gauged $U(1)_l$ lepton model was constructed to study the nature of lepton number. Different from previous studies in the literature, we found two solutions which are free of the anomaly for each SM fermion generation. Our solutions also do not require type I see-saw mechanism for active neutrino mass generation. The price we pay is to introduce four extra chiral fermion fields per generation. While the two solutions whose anomaly cancelation is nontrivial, look superficially similar. The fermion content of one solution is displayed in Tab.I. We have constructed the minimal scalar sector, Tab.II, such that the active neutrino masses are generated radiatively without significant fine-tuning the model parameters. Moreover, the new leptons acquire their masses from the vacuum expectation values of SM Higgs doublet and the scalars, $\phi_{1,2}$, which carry nonzero lepton numbers.

An immediate phenomenological consequence is the existence of a new gauge boson, Z_l , which is universal for any gauged $U(1)_l$ model. The mass of Z_l , M_X , is determined by the lepton charges of the scalars $\phi_{1,2}$ and the lepton number violating VEVs, $\langle\phi_{1,2}\rangle$. The Z_l boson interferes with the SM photon and Z -boson in the process $e^+e^- \rightarrow l\bar{l}$. Even if the center-of-mass energy of the e^+e^- collider is below the mass of Z_l , its effects can be unambiguously identified from the Z line shape and the forward-backward asymmetries. This can be seen in Fig.1 and Fig.2. In contrast, the front-back asymmetries of the quarks will not change from their SM values. The combination of these two measurements will shed light on the nature of any extra Z boson.

As noted previously, Z_l can be produced at a hadron collider by radiating from a lepton line from the usual Drell-Yan process via the reaction $pp \rightarrow \ell\bar{\ell}\ell'\bar{\ell}'$ with the invariant mass of one pair of leptons, $\ell\bar{\ell}$ say, peaking at M_X . The final state to look for are four leptons with no jets. We found that the LHC14, LHC30, and LHC100 with an integrated luminosity $3000(fb)^{-1}$ can probe the

lepton number violating scale up to roughly 0.5, 1.0, and 2.0 TeV, respectively. This is the same range of direct Z_ℓ production can be reached at the e^+e^- colliders such as ILC500 and CLIC at 2 TeV. The latter also provides much cleaner environment. For the constraint on the coupling for a light scenario-(B)-type Z_ℓ , see [35].

Since the SM fermions content is anomalous under $U(1)_\ell$, new heavy leptons are mandated to cancel the anomaly for a UV complete theory. The masses of these exotic leptons are usually free parameters and can be heavier than the reach of any foreseeable colliders. We studied the phenomenologically more interesting case where their masses are < 1.0 TeV. The production of the heavy charged lepton pair at an e^+e^- collider is $\sim O(10 - 10^2)fb$, and the signals for their detection can be very clean. Due to the negligible mixing of E, N with their SM counter parts, the usual detection channels do not apply. For example, for a heavy neutrino N , the usual detection channel is $N \rightarrow eW$. However, for our solution N predominantly decays into final states with $W + 3\ell$ (see Eqs.(86),(87)). We have used the result that $h_1(a_1)$ will have sizable couplings to SM charged leptons with $Y_1 \gtrsim 0.1$.

The production and detection at a hadron collider is much more complicated. At the LHC while the cross sections are not too small, i.e. $O(1 - 10^2)fb$ for $M_E, M_N < 500$ GeV. But one needs a comprehensive study of the SM backgrounds for each possible final state. For a heavy neutrino with the usual decay this has been extensively studied before[36]. Our preferred final states are different and typically involve multi-leptons and no accompany jet activities other than hadronic W . We shall leave such a

comprehensive study to future work. We note that multi-lepton signals at the LHC were investigated in [37–39] for various scenarios and different models.

Moreover, we have also studied the imprints of the new scalars and heavy leptons at low energies. It is found that the most prominent constraint on the new fields is from the oblique parameters, ΔS and ΔT . We have carefully studied the current experimental bounds on ΔS and ΔT and the direct searches for the new charged scalar and heavy charged lepton as well. The electroweak precision bounds require that the new heavy leptons have to be nearly degenerate. This is a generic feature of any gauged $U(1)_\ell$ model with the custodial symmetry, nearly degenerate new $SU(2)$ doublet leptons will occur. Depending on their masses, the mass splitting between the heavy neutrino and charged lepton has to be less than $O(1 - 10\%)$. This will severely constrain the parameters of the model. We look forward to future improvements on the measurements of these quantities.

ACKNOWLEDGMENTS

WFC is supported by the Taiwan Minister of Science and Technology under Grant Nos. 106-2112-M-007-009-MY3 and 105-2112-M-007-029. WFC thanks the hospitality of Prof. Chi-Ting Shih and the Department of Applied Physics of Tunghai University where part of his work is done. TRIUMF receives federal funding via a contribution agreement with the National Research Council of Canada and the Natural Science and Engineering Research Council of Canada.

-
- [1] S. Weinberg, Phys. Rev. Lett. **43**, 1566 (1979).
 - [2] S. L. Glashow, *Cargese Summer Institute: Quarks and Leptons Cargese, France, July 9-29, 1979*, NATO Sci. Ser. B **61**, 687 (1980); T. Yanagida, *Proceedings: Workshop on the Unified Theories and the Baryon Number in the Universe: Tsukuba, Japan, February 13-14, 1979*, Conf. Proc. **C7902131**, 95 (1979); R. N. Mohapatra and G. Senjanovic, Phys. Rev. Lett. **44**, 912 (1980), [231(1979)]; J. Schechter and J. W. F. Valle, Phys. Rev. **D25**, 774 (1982).
 - [3] W.-F. Chang, J. N. Ng, and J. M. S. Wu, Phys. Lett. **B730**, 347 (2014), arXiv:1310.6513 [hep-ph].
 - [4] W.-F. Chang and J. N. Ng, Phys. Rev. **D90**, 065034 (2014), arXiv:1406.4601 [hep-ph].
 - [5] W.-F. Chang and J. N. Ng, JCAP **1607**, 027 (2016), arXiv:1604.02017 [hep-ph].
 - [6] T. D. Lee and C.-N. Yang, Phys. Rev. **98**, 1501 (1955).
 - [7] L. Okun, Phys. Lett. **B382**, 389 (1996), arXiv:hep-ph/9512436 [hep-ph].
 - [8] P. Fileviez Perez and M. B. Wise, Phys. Rev. **D82**, 011901 (2010), [Erratum: Phys. Rev. **D82**, 079901(2010)], arXiv:1002.1754 [hep-ph].
 - [9] P. Schwaller, T. M. P. Tait, and R. Vega-Morales, Phys. Rev. **D88**, 035001 (2013), arXiv:1305.1108 [hep-ph].
 - [10] M. Magg and C. Wetterich, Phys. Lett. **94B**, 61 (1980); G. Lazarides, Q. Shafi, and C. Wetterich, Nucl. Phys. **B181**, 287 (1981); R. N. Mohapatra and G. Senjanovic, Phys. Rev. **D23**, 165 (1981); T. P. Cheng and L.-F. Li, Phys. Rev. **D22**, 2860 (1980).
 - [11] W. Chao, Phys. Lett. **B695**, 157 (2011), arXiv:1005.1024 [hep-ph].
 - [12] B. Fornal, Y. Shirman, T. M. P. Tait, and J. R. West, Phys. Rev. **D96**, 035001 (2017), arXiv:1703.00199 [hep-ph].
 - [13] B. Holdom, Phys. Lett. **166B**, 196 (1986); Phys. Lett. **B259**, 329 (1991).
 - [14] W.-F. Chang, J. N. Ng, and J. M. S. Wu, Phys. Rev. **D74**, 095005 (2006), [Erratum: Phys. Rev. **D79**, 039902(2009)], arXiv:hep-ph/0608068 [hep-ph].
 - [15] G. Aad *et al.* (ATLAS, CMS), JHEP **08**, 045 (2016), arXiv:1606.02266 [hep-ex].
 - [16] H. Baer, T. Barklow, K. Fujii, Y. Gao, A. Hoang, S. Kanemura, J. List, H. E. Logan, A. Nomerotski, M. Perelstein, *et al.*, (2013), arXiv:1306.6352 [hep-ph].

- [17] P. Lebrun, L. Linssen, A. Lucaci-Timoce, D. Schulte, F. Simon, S. Stapnes, N. Toge, H. Weerts, and J. Wells, (2012), 10.5170/CERN-2012-005, arXiv:1209.2543 [physics.ins-det].
- [18] S. Schael *et al.* (DELPHI, OPAL, LEP Electroweak, ALEPH, L3), Phys. Rept. **532**, 119 (2013), arXiv:1302.3415 [hep-ex].
- [19] A. Leike, T. Riemann, and J. Rose, Phys. Lett. **B273**, 513 (1991), arXiv:hep-ph/9508390 [hep-ph]; T. Riemann, Phys. Lett. **B293**, 451 (1992), arXiv:hep-ph/9506382 [hep-ph].
- [20] M. Bicer *et al.* (TLEP Design Study Working Group), *Proceedings, 2013 Community Summer Study on the Future of U.S. Particle Physics: Snowmass on the Mississippi (CSS2013): Minneapolis, MN, USA, July 29-August 6, 2013*, JHEP **01**, 164 (2014), arXiv:1308.6176 [hep-ex]; D. d’Enterria, *Proceedings, Physics Prospects for Linear and other Future Colliders after the Discovery of the Higgs (LFC15): Trento, Italy, September 7-11, 2015*, Frascati Phys. Ser. **61**, 17 (2016), arXiv:1601.06640 [hep-ex].
- [21] C.-S. S. Group, “CEPC-SPPC Preliminary Conceptual Design Report. 1. Physics and Detector,” (2015).
- [22] C. Patrignani *et al.* (Particle Data Group), Chin. Phys. **C40**, 100001 (2016).
- [23] P. L. Anthony *et al.* (SLAC E158), Phys. Rev. Lett. **95**, 081601 (2005), arXiv:hep-ex/0504049 [hep-ex].
- [24] A. Belyaev, N. D. Christensen, and A. Pukhov, Comput. Phys. Commun. **184**, 1729 (2013), arXiv:1207.6082 [hep-ph].
- [25] J. Pumplin, D. R. Stump, J. Huston, H. L. Lai, P. M. Nadolsky, and W. K. Tung, JHEP **07**, 012 (2002), arXiv:hep-ph/0201195 [hep-ph].
- [26] M. E. Peskin and T. Takeuchi, Phys. Rev. Lett. **65**, 964 (1990).
- [27] M. E. Peskin and T. Takeuchi, Phys. Rev. **D46**, 381 (1992).
- [28] G. Aad *et al.* (ATLAS), JHEP **09**, 108 (2015), arXiv:1506.01291 [hep-ex].
- [29] W.-F. Chang, T. Modak, and J. N. Ng, Phys. Rev. **D97**, 055020 (2018), arXiv:1711.05722 [hep-ph].
- [30] W.-F. Chang, J. N. Ng, and G. White, (2018), arXiv:1803.00148 [hep-ph].
- [31] A. Djouadi, Phys. Rept. **457**, 1 (2008), arXiv:hep-ph/0503172 [hep-ph].
- [32] A. M. Sirunyan *et al.* (CMS), (2018), arXiv:1804.02716 [hep-ex].
- [33] W.-F. Chang, J. N. Ng, and J. M. S. Wu, Phys. Rev. **D86**, 033003 (2012), arXiv:1206.5047 [hep-ph].
- [34] R. Barate *et al.* (OPAL, DELPHI, LEP Working Group for Higgs boson searches, ALEPH, L3), Phys. Lett. **B565**, 61 (2003), arXiv:hep-ex/0306033 [hep-ex].
- [35] Y. S. Jeong, C. S. Kim, and H.-S. Lee, Int. J. Mod. Phys. **A31**, 1650059 (2016), arXiv:1512.03179 [hep-ph].
- [36] J. N. Ng, A. de la Puente, and B. W.-P. Pan, JHEP **12**, 172 (2015), arXiv:1505.01934 [hep-ph].
- [37] J. A. Aguilar-Saavedra, Nucl. Phys. **B828**, 289 (2010), arXiv:0905.2221 [hep-ph].
- [38] C.-Y. Chen and P. S. B. Dev, Phys. Rev. **D85**, 093018 (2012), arXiv:1112.6419 [hep-ph].
- [39] N. Arkani-Hamed, K. Blum, R. T. D’Agnolo, and J. Fan, JHEP **01**, 149 (2013), arXiv:1207.4482 [hep-ph].